Mineral. Deposita 31, 407–418 (1996)

MINERALIUM DEPOSITA

Physicochemical conditions of deposition and origin of carbonate-hosted base metal sulfide mineralization, Thermes ore-field, Rhodope Massif, northeastern Greece

S.I. Kalogeropoulos[1], S.P. Kilias[2], N.D. Arvanitidis[2]

[1] Rusvar Holdings BV, 4 Nikis St., 105 62 Athens, Greece
[2] Institute of Geology and Mineral Exploration (IGME), 1 Fragon St., 546 26 Thessaloniki, Greece

Received: 19 January 1995/Accepted: 20 March 1996

Abstract. Vein and stratabound base metal sulfide mineralization of the Thermes ore-field, Rhodope Massif, NE Greece, is hosted in marbles. The Thermes area is a structurally complex, E–W-trending zone consisting of felsic gneisses alternating with amphibolites, amphibole-biotite, and biotite gneisses, and marbles. These rocks have undergone amphibolite facies metamorphism (5–7 kbar, 580 °–620 °C), in Upper Cretaceous to Eocene times, and were subsequently retrograded to greenschist facies metamorphism of Miocene age. Granitoids of Oligocene age, and volcanic rocks of Eocene-Oligocene age, crosscut the metamorphic rocks. Two major base metal sulfide ore varieties occur in the Thermes ore-field. The first comprises brecciated vein Pb-Zn mineralization, related to NNW- and NNE-trending faults. The second comprises stratabound (manto) polymetallic, and Pb-Zn replacement ores with associated veins. On the basis of ore geochemistry, as well as field and textural evidence, these two ore varieties form part of a vein associated skarn-replacement base metal sulfide ore system. Based on fluid inclusion data in quartz, together with the iron content of sphalerites and existing lead and sulfur isotope data, it is suggested that after the cessation of the regional amphibolite facies metamorphism circulating evolved meteoric waters, probably with magmatic fluid contributions, deposited sulfide ores at temperatures of 200 °–400 °C, and pressures of less than 300 bar. Ore was deposited as a result of increase in pH of the mineralizing fluids due to fluid-rock interaction, and adiabatic cooling and/or simple cooling accompanying fluid boiling. Thermochemical considerations indicate a pH increase from about 4 to 7 and a decrease in f_{S_2} and f_{O_2}.

The Thermes base metal sulfide ore-field occurs in the central part of the polymetamorphic and structurally complex Rhodope Massif (RM), and forms the southern extension of the Madan base metal ore-field located in Bulgaria (Fig. 1). A number of studies dealing with various aspects of the sulfide ores have been published (e.g., Kalogeropoulos and Arvanitidis 1989; Arvanitidis et al. 1989 a, b; Arvanitidis and Dimou 1990; Changkakoti et al. 1990). However, except for sulfur and lead isotopic studies (Changkakoti et al. 1990), no other data pertinent to the physicochemical conditions of ore deposition have been published.

The present study combines chemical, fluid inclusion, and published isotopic data, in an attempt to determine the physicochemical conditions of deposition, elucidate the ore-forming processes, and to assist in refining an exploration strategy for these and other similar deposits in the region.

Geology of the Thermes base metal sulfide ore-field

The Thermes ore-field is hosted by a structurally complex E–W trending zone within the RM. The RM includes Pre-Devonian to Mesozoic rocks and occupies most of northeastern Greece and southern Bulgaria. To the west, the RM is separated from the Servo-Macedonian Massif by the Strimon River fracture zone, whereas the RM is bounded to the S–SE by the Triassic-Jurassic Circum-Rhodope Belt (CRB). The geology of the RM, and CRB, has been recently summarized by Von Braun (1993).

Base metal sulfide mineralization in the Thermes ore-field is controlled regionally by NNW and NNE fault directions and the presence of marble lithologies (Fig. 1). Marbles occur both in a lower "autochthon" unit (>700 m thick) comprised of felsic gneisses with minor amphibolites, biotite-gneisses, and locally migmatites, and an upper "allocthon" unit (400–600 m thick) consisting of alternations of marbles and amphibole-gneisses, which are infrequently invaded by pegmatites. These two units are separated by a major Tertiary, low-angle (10–30°) thrust fault. Geochemical studies of protoliths suggest that the gneisses were derived mainly from igneous rocks of calc-alkaline affinity (Mposkos et al. 1990; Arvanitidis et al. 1989a) whereas most of the amphibolites were interpreted as tholeiites, bearing both island arc and MORB signatures (Mposkos et al. 1990).

The rocks in the Thermes area have been deformed and metamorphosed regionally to the amphibolite facies at pressures of 5 to 7 kbar and temperatures between 580° and 620 °C (Arvanitidis et al. 1989a).

Correspondence to: S.P. Kilias

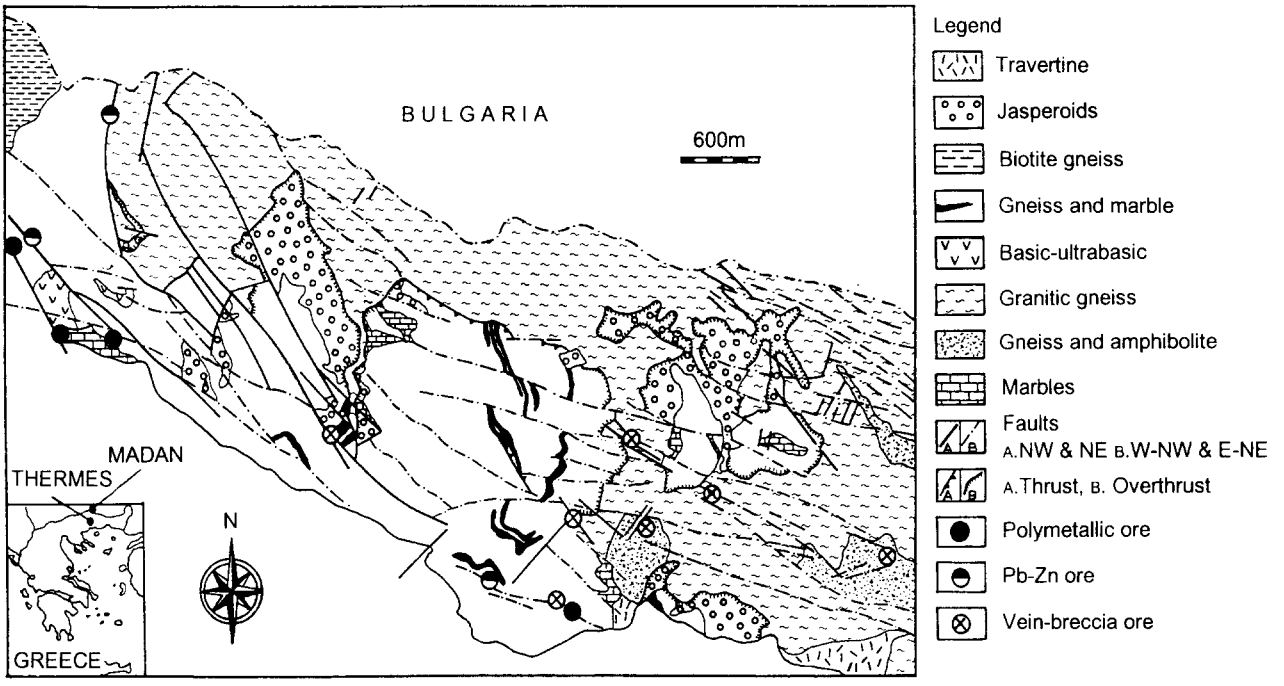

Fig. 1. Geology of the Thermes ore field (modified after Manev et al. 1990)

This prograde metamorphism probably spans Upper Cretaceous (Yordanov et al. 1962) to Eocene age (45–50 Ma, K\Ar age of hornblende in amphibolites, Liati 1986) and was overprinted by retrograde greenschist facies metamorphism of Miocene age (13.9–15.9 Ma, Kyriakopoulos 1987, and 15.5–17.8 Ma, Kokkinakis 1980).

Metamorphic rocks in the vicinity of Thermes were intruded by Oligocene granitoids of calc-alkaline affinity (i.e., Xanthi, 26.3–28.8 Ma-whole rock Rb/Sr age, Kyriakopoulos (1987); 27.1–27.9 Ma-K/Ar biotite age, Meyer (1968); and Paranesti, 29.1–38.5 Ma-K/Ar biotite age, Sklavounos (1981); 38.3 Ma-K/Ar muscovite age, Meyer (1968). Volcanic rocks occur both in Eocene to Oligocene (37–25 Ma) basins (Fytikas et al. 1985; Eleftheriadis et al. 1989) and along linear structures in the metamorphic terrane (Alfieris et al. 1989).

In an earlier study of the mineralization, Arvanitidis et al. (1986) observed a lateral variation in sulfide mineral associations from high-T skarn ores, near the Oligocene volcanics, to low-T vein/replacement ores. The present study concerns vein/replacement ores only.

On the basis of mode of occurrence and morphology, as well as chemical character, ore mineralogy and alteration features, two major ore varieties were recognized (Arvanitidis et al. 1986, 1989b): (1) a fault-related, breccia Pb-Zn (Fe-Cu) mineralization; (2) strata-bound, replacing marbles with extensions to mineralized veins in faults (Fig. 2). The latter variety is subdivided into polymetallic (Zn-Pb-Fe-Cu-As-Ag-Au-Cd-Sb) and Pb-Zn (Cu-Mn-Ag-Cd) types. Main mineral assemblages of both major types consist of coexisting sphalerite, galena, pyrite with quartz, sericite and carbonates gangue; chalcopyrite also occurs in subordinate amounts. Arsenopyrite is present in the polymetallic ore variety only. Descriptions of ore mineralogy, gangue minerals and hydrothermal alteration are presented in Arvanitidis and Dimou (1990).

Cu-Pb-Zn and Cu-(Pb+Zn)-Ag × 10^3 relations

Various types of Pb-Zn (Cu) deposits that occur in distinct geological settings are characterized by different metal ratios. Such ratios have been utilized to indicate possible genetic links among them (e.g., Sangster and Scott 1976; Franklin et al. 1981; Gustafson and Williams 1981). Figure 3 shows plots of the bulk composition of the three Thermes ore varieties in terms of their Cu-Pb-Zn (Fig. 3A) and Cu-(Pb+Zn)-Ag × 10^3 contents (Fig. 3B). For comparison, the ternary plots also show the data fields for worldwide base metal sulfide sediment-hosted and volcanogenic deposits, as well as 12 Pb-Zn skarn-replacement deposits. These data indicate a similarity between the base metal and Ag compositions of the Thermes ores and worldwide sediment-hosted and skarn-replacement ores.

Sphalerite chemistry

Sphalerite exhibits a wide range of optical and chemical variations that can provide information concerning conditions of deposition and metamorphism (Barton and Toulmin 1966; Scott and Barnes 1971). The chemical composition of sphalerite coexisting with pyrite was determined utilizing a JEOL Superprobe 733 (Table 1). Operating conditions included an operating voltage of 20 kV, a beam current of 5nA and 20 second count times. Mineral standards were used, and on line ZAF corrections were carried out using a PDP-11/04 computer. The error in the iron content of sphalerite is less than 0.2 mol % FeS.

On statistical grounds (student t-test), the mean Fe content shows an increase from the breccia/vein, to the replacement Pb-Zn, to the polymetallic replacement ore variety. Manganese does not show any statistically significant difference between the latter two varieties, however it is lower in the former. Finally Cd forms a single population for all three varieties.

In most cases, the iron content of single sphalerite grains and between grains of the same sample is variable

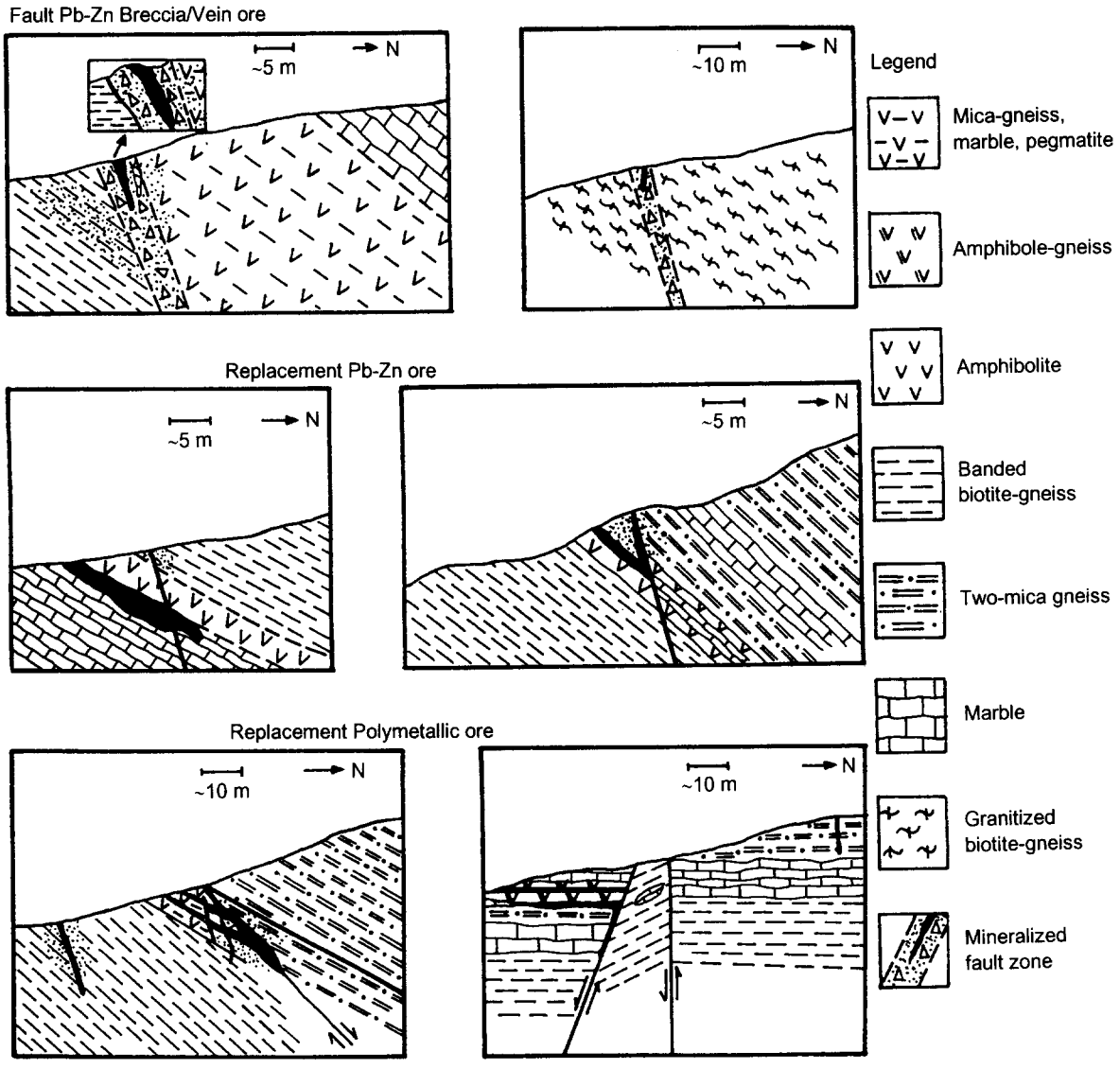

Fig. 2. Generalized cross sections of the Thermes mineralization types

and related to chromatic variations. The greatest variability in mol % FeS of the centers and the margins within single grains and between grains was found in sphalerites from the polymetallic variety, whereas sphalerties from the breccia/vein variety do not exhibit any major chemical and chromatic zonation. Such variations indicate that fluctuations in the activity of FeS in the mineralizing fluid and/or the temperature and fugacity of sulfur at deposition were more pronounced in the polymetallic ore variety.

Fluid inclusion study

Fluid inclusions were studied in quartz and sphalerite from 18 samples representing replacement polymetallic (5), replacement Pb-Zn (10) and breccia/vein Pb-Zn (3) sulfide ore varieties. Microthermometry was conducted using 100–200 μm thick doubly polished chips utilizing a Linkam TH600 heating-freezing stage connected to a Linkam TMS90 programmer. The operation of the stage has been described by Shepherd (1981). The stage was calibrated in the range $-92\,^{\circ}C$ to $+592\,^{\circ}C$ using the method of Macdonald and Spooner (1981). The uncertainty in the heating and freezing measurements is $\pm 0.5\,^{\circ}C$.

It should be noted that the Fe-As-S system (Kretshmar and Scott 1976) was not employed for an independent check on formation temperatures, as arsenopyrite compositional data were not obtained due to its limited occurrence in the replacement polymetallic ore variety only.

Nature of fluid inclusions

The fluid inclusions studied by microthermometry were identified as primary using the criteria of Roedder (1984). Primary inclusions occur in random clusters with no

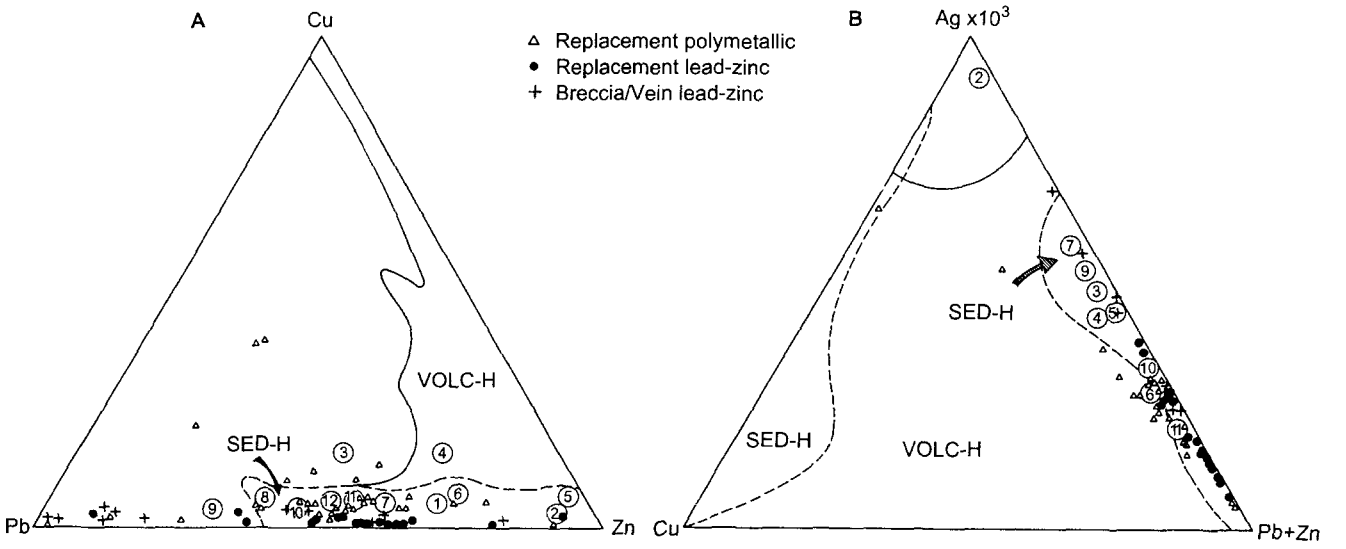

Fig. 3. **A** Comparison of the bulk Cu-Pb-Zn, and B Cu-(Pb + Zn)-Ag × 10^3 compositions of the sediment-hosted (SED-H), volcanic-hosted (VOLC-H), and skarn Pb-Zn sulfide ore types with the Thermes ore varieties. Data for the former two types in **A** are from Lydon (1983) and in **B** are from Gustafson and Williams (1981). Data for skarn-type Pb-Zn sulfide ores shown in *circled numbers* are from Einaudi et al. (1981): 1, Ulchin, Korea; 2, Yeonhua II, Korea; 3, Henpaoshan-Sikarg province, hina; 4, Groundhog, New Mexico, USA; 7, Frisco, Mexico; 8, Hidalgo, Mexico; 9, Stri Trig Trepca, Yugoslavia; 10, Aravaipa, Arizona, USA; 11, Bluebell, Canada; 12, Uchucchacua, Peru

Table 1. Sphalerite chemistry for the Thermes ore varieties

Elements	Replacement						Breccia/vein		
wt. %	Polymetallic $n = 28$			Pb-Zn $n = 49$			Pb-Zn $n = 11$		
	$\bar{x}$	1σ	Range	$\bar{x}$	1σ	Range	$\bar{x}$	1σ	Range
Zn	60.5	0.7	58.7–61.9	62.5	2.0	56.3–65.4	66.4	0.9	65.2–68.2
Fe	5.0	0.8	3.4–6.5	3.1	1.5	1.4– 9.1	0.6	0.3	0.2– 1.1
Cu	–	–	–	–	–	–	–	–	–
Mn	1.3	0.3	0.5–1.8	1.3	0.3	0.7– 2.0	0.4	0.2	0.2– 0.7
Cd	0.3	0.3	0.05–1.1	0.2	0.2	0.02–0.6	0.3	0.2	0.01–0.6
S	32.8	0.4	32.0–33.5	32.7	0.4	31.4–33.9	32.5	0.7	31.4– 33.3
Total	99.9			99.8			100.2		
Mol %									
FeS	8.5	1.4	5.8–11.6	5.3	2.6	2.4–15.4	0.8	0.5	0.3– 1.9
MnS	2.3	0.5	0.9– 3.0	2.3	0.6	1.2– 3.5	0.7	0.4	0.2– 1.6
CdS	0.2	0.2	0.01–0.7	0.1	0.1	0.01–0.5	0.2	0.2	0.01–0.4

$\bar{x}$: mean 1σ: standard deviation

obvious internal arrangement or they are isolated (Fig. 4). Fracture-related secondary inclusions were avoided in the present study. Two types of inclusions were distinguished:

Type I inclusions contain liquid and a vapor bubble that comprises 20–40% of the total inclusion volume (Fig. 4). They homogenize to the liquid phase. Accidentally trapped irregular opaque solid phases were occasionally observed.

Type II inclusions contain liquid and a vapor bubble occupying between 50 and 90 vol.% of the inclusion (Fig. 4). They homogenize to the vapor phase or, in rare cases, show critical homogenization. Daughter minerals were not observed in this study.

Most inclusions range from 10 to 20 μ in their longest dimension and have elliptical to rounded shapes. Liquid-rich and vapor-rich inclusions commonly occur together in quartz from samples of the polymetallic ore variety (Fig. 4), suggesting the presence of two immiscible phases, vapor and liquid, due to boiling at the time of inclusion formation. The absence of single-phase liquid filled inclusions in the vicinity of vapor-rich inclusions supports the suggestion that these inclusions trapped a vapor phase and that they are not the result of necking processes (Bodnar et al. 1985b). The majority of inclusions in sphalerite are either opaque due to internal reflections, or have been "necked down". Those sphalerite-hosted

inclusions in which vapor bubbles were visible, resemble type I inclusions in quartz. Although "necked down" inclusions were avoided in microthermometric studies it is unclear whether or not some measured inclusions were the result of "necking down". No measurable inclusions were observed in sphalerite crystals from samples of breccia/vein ores.

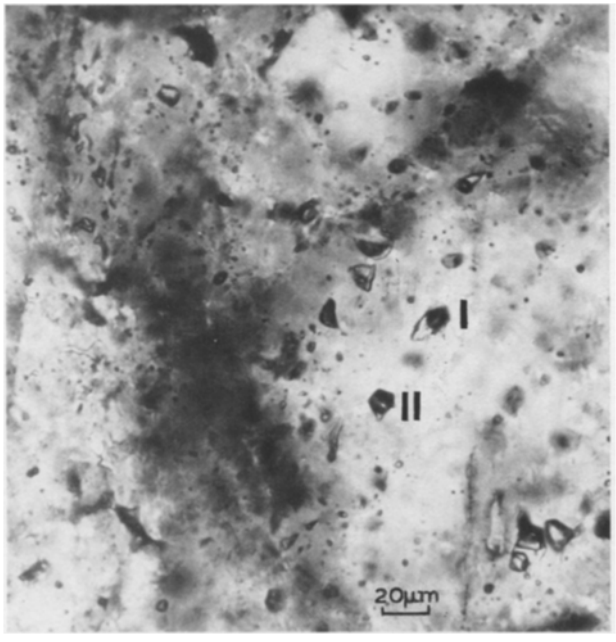

Fig. 4. Random distribution of co-existing primary liquid-rich (type I) and vapor-rich (type-II) inclusions in quartz from the polymetallic ore variety

Microthermometry results and interpretation

Homogenization temperatures (T_h). type I inclusions in quartz homogenize at temperatures between 154° and 328 °C (Fig. 5A, C, D). Ranges of T_h values for each variety of ore are: replacement polymetallic, 154°–382 °C; replacement Pb-Zn, 309°–361 °C; breccia/vein, 196°–320 °C. Histograms of the T_h data display identifiable peaks at: 180° ±10 °C and 340° ±20 °C (polymetallic ore) (Fig. 5A), 350° ±10 °C (Pb-Zn ore) (Fig. 5C), and 230° ± 10 °C and 310° ± 10 °C (breccia/vein ore) (Fig. 5D). The 340° ± 20 °C peak of the polymetallic ore corresponds very well to the 350° ± 10 °C peak of the Pb–Zn ore. T_h values for polymetallic ore display a wide range, and are separated into two distinct groups (Fig. 5A). This most likely reflects a series of two hydrothermal episodes rather than one specific event. The T_h values of type II inclusions range from 332° to 385 °C (Fig. 5B) and cluster around a median value of 365 °C. Overlapping T_h values of coexisting type I and type II inclusions between 330° and 380 °C, in samples of polymetallic ore (Fig. 5A, B), coupled with contrasting homogenization mode to the liquid and vapor phases, respectively, support the concept that fluid immiscibility may have occurred periodically during polymetallic ore deposition.

Fluid inclusion T_h values for the replacement Pb-Zn ores overlap with the higher T_h population obtained from

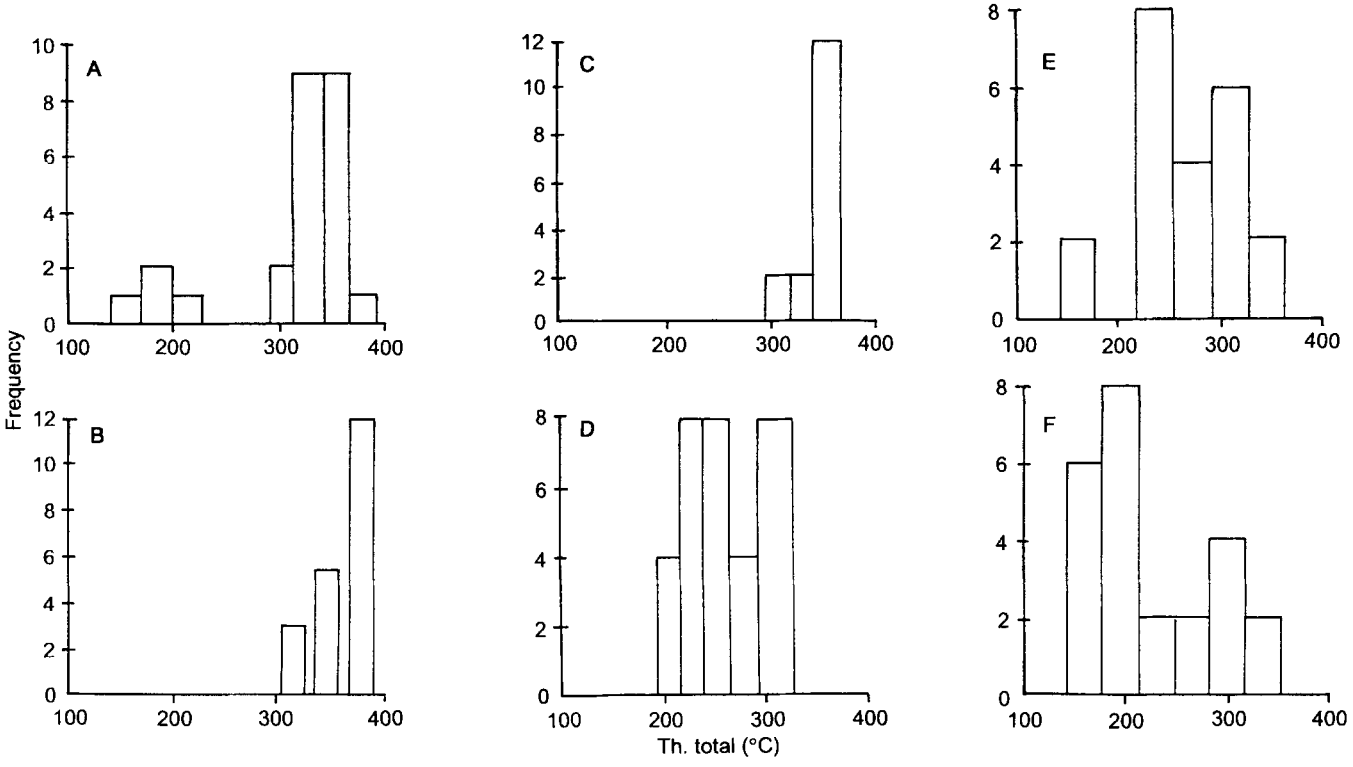

Fig. 5A–F. Histograms of homogenization temperatures, T_h, of quartz-hosted inclusions from replacement polymetallic [**A**: homogenization to liquid (type I); **B**: homogenization to vapor (type II)], replacement Pb-Zn (type I) **C**, and breccia/vein (type I) **D** ores, and sphalerite-hosted type I inclusions from the replacement polymetallic **E**, and Pb-Zn **F** ores

the replacement polymetallic ore (Fig. 5A, C) strongly suggesting that these ore varieties were coeval, and represent mineralogically different aspects of the same ore-forming system. Homogenization temperature data from the breccia/vein ore form a continuum from 196° to 320 °C, and part of this range, centered around 310° ± 10 °C, overlaps with T_h values from the two replacement ore varieties (Fig. 5A, C, D). These temperature data suggest that the breccia/vein ore is part of the same ore-forming system that deposited the replacement ores and followed, the waning stages of the thermal evolution of replacement ore-deposition.

Sphalerite from the polymetallic (Fig. 5E) and Pb-Zn (Fig. 5F) ores show a wide scatter of type I inclusion T_h values from 175° to 337 °C, probably resulting from "necking down".

Melting temperatures and composition of inclusion fluids. Ice melting temperatures (Tm, ICE), of type I inclusions, from all ore varieties, varied from − 19.6° to − 2.0 °C (Fig. 6A) Most quartz-hosted inclusions exhibited melting temperatures of greater than − 6 °C (Fig. 6A, B, C). The range for most sphalerite-hosted inclusions was between − 8 °C and − 5 °C (Fig. 6D). Initial melting temperatures (eutectic melting were difficult to observe due to the small size of the inclusions. However, a few estimates of eutectic temperatures ranged from − 25° to − 22 °C indicating that some inclusions likely contained KCl in addition to NaCl (Crawford 1981). Carbon dioxide clathrate melting was not observed in any type I inclusions, limiting their possible CO_2 content to less than 0.85 *m*.

Owing to the small proportion of liquid, and the small size of the inclusions, melting phenomena could only be observed in a very small number of type II inclusions. Freezing tests produced double freeze phenomena (Collins 1979) at temperatures below − 35 °C and − 100 °C corresponding to ice and, in all probability, solid CO_2, respectively. Melting of the low temperature solid could be observed in few cases at temperatures very close to − 57 °C confirming the presence of frozen CO_2 in the inclusions. It is thus strongly indicated that the vapor bubble in type II inclusions consists of $H_2O + CO_2$. Final melting (ice?) could only be observed in three inclusions at temperatures between − 2.5° and − 0.7 °C.

Salinities of type I inclusions in quartz were calculated in the system H_2O-NaCl based on ice-melting temperatures (Potter et al. 1978) (Fig. 6), and range from: 3.5 to 22.4 wt.% NaCl equivalent (replacement polymetallic); 5.3

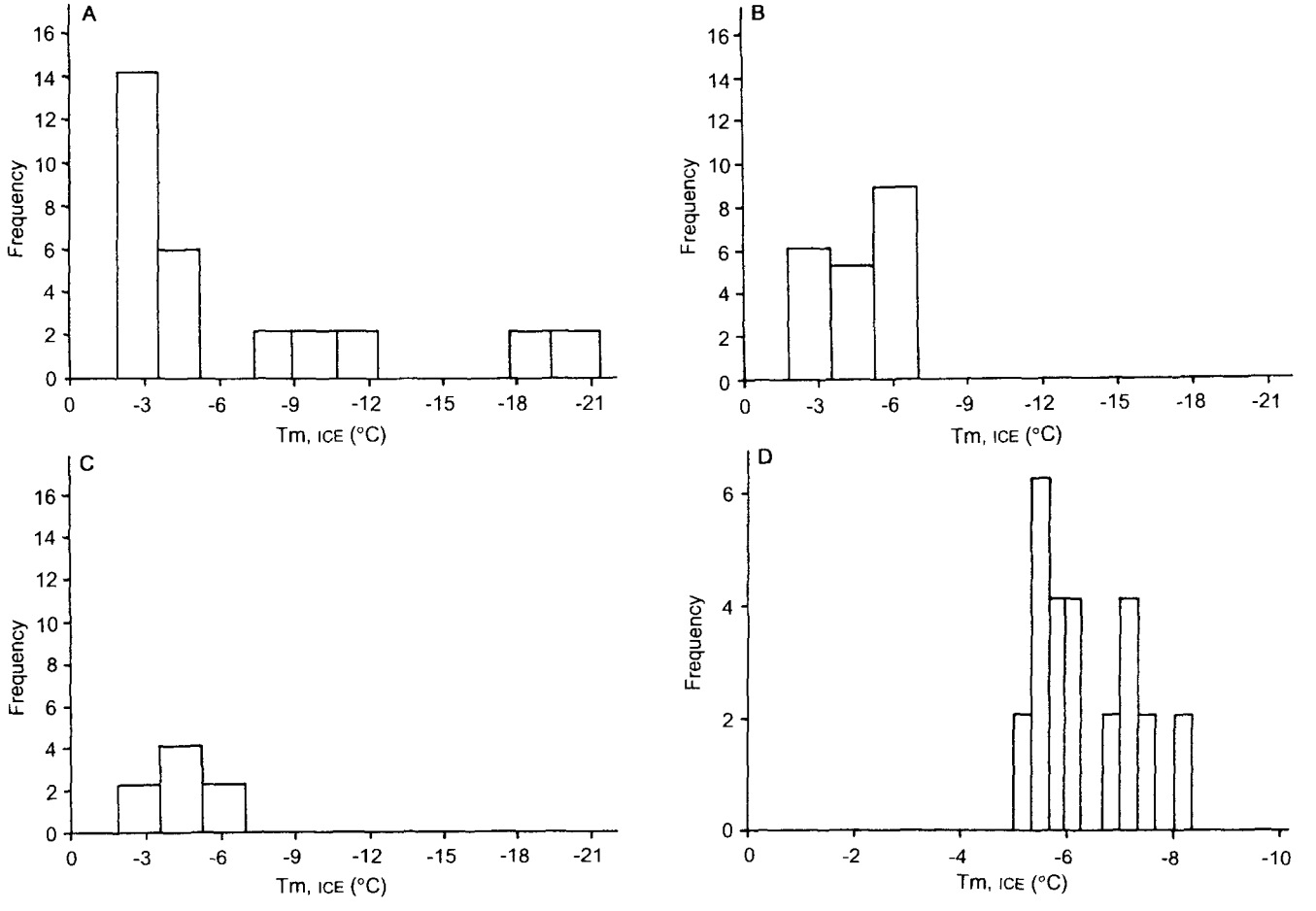

Fig. 6A–D. Histograms of ice-melting temperatures, T_m, ICE, of quartz-hosted type I inclusions from replacement polymetallic **A**, replacement Pb-Zn **B** and breccia/vein **C** ores, and sphalerite-hosted type I inclusions, from replacement polymetallic and replacement Pb-Zn ores **D**

Table 2. Microthermometry data and properties of type I and type II inclusions.[a]

Ore type	Inclusion type Mineral	Ice melting Tm, ICE (°C)	Salinity (Equivalent wt.% NaCl)	temperatures Homogenization *Th* (°C)	Bulk density (g/cm^3)
Replacement Polymetallic	I Quartz	R: −19.6 to 2.0 X: −6.5 ± 5.0 M: −3.7	R:3.5 − 22.4 X:10.5 ± 5.4 M:6.4	R:154 − 382 X:320 ± 62 M:339	R:0.65 − 1.07 X:0.79 ± 0.15 M:0.74
	II Quartz	R: −2.5 to −0.7 X: −1.6 ± 0.3 M: −1.3	R:1.0 − 3.5 X:2 ± 0.5 M:2.0	R:332 − 386 X:366 ± 18 M:370	–
	I Sphalerite	R: −7.0 to −4.7 X: −5.7 ± 0.7 M: −5.0	R:8.1 − 11.1 X:9.7 ± 1 M:9.7	R:176 − 337 X:233 ± 57 M:212	R:0.78 ± 0.97 X:0.89 ± 0.07 M:0.89
Replacement Pb-Zn	I Quartz	R: −6.3 to −3.2 X: −4.9 ± 1.2 M: −5.5	R:5.2 − 9.6 X:7.1 ± 1.7 M:6.3	R:309 − 361 X:346 ± 16 M:350	R:0.68 − 0.75 X:0.70 ± 0.03 M:0.68
	I Sphalerite	R: −7.7 to 5.0 X: −5.6 ± 1.2 M: −5.6	R:8.5 − 11.6 X:9.3 ± 1.3 M:8.5	R:174 − 333 X:264 ± 44 M:256	R:0.89 ± 0.91 X:0.88 ± 0.02 M:0.87
Breccia/Vein	I Quartz	R: −6.3 to −3.2 X: −5.1 ± 1.4 M: −5.0	R:6.0 − 10.0 X:8.2 ± 1.8 M:8.0	R:196 − 320 X:269 ± 36 M:266	R:0.73 − 0.95 X:0.87 ± 0.06 M:0.88

[a] Data are from Figs. 5 and 6; R: range, X: average, ± standard deviation, M: median

to 9.6 wt.% NaCl equivalent (replacement Pb-Zn); 6.0 to 10.0 wt.% NaCl equivalent (breccia/vein). Sphalerite-hosted inclusions have a more restricted salinity range between 5.3 and 9.6 wt.% NaCl equivalent. Melting phenomena in type II inclusions correspond to salinities of the liquid phase between 1 and 3.5 wt.% NaCl equivalent (Potter et al. 1978). It should be noted that the reported salinities represent maximum values because freezing point depression up to −1.5 °C could be due to up to 0.85 *m* dissolved CO_2 without clathrate behavior during freezing (Hedenquist and Henley 1985). Therefore, the reported salinities may be higher, by up to 2.5 wt.% NaCl equivalent and type I inclusions may contain a maximum of undetected 0.85 *m* CO_2. Salinity determinations and calculated inclusion bulk densities, for inclusion types I and II, are summarized in Table 2, along with microthermometry data. Inclusion bulk densities were calculated using the computer program, FLINCOR (Brown 1989).

Salinity versus homogenization temperature relations. Variations in salinity versus T_h values of type I inclusions from all three ore varieties are illustrated in Fig. 7. Periodic immiscibility during polymetallic mineralization indicates that type I and type II inclusions in quartz of the polymetallic ore may represent immiscible phases trapped in the course of unmixing of a homogeneous fluid. Saline-H_2O and CO_2 are known to be immiscible over a wide range of temperature, pressure and salinities (Bowers and Helgeson 1983; Brown and Lamb 1989). Arrow number 1 shown in the inset diagram of Fig. 7 represents a "boiling" trend described by Shepherd et al. (1985). During the process of phase unmixing the liquid phase (recorded in type I inclusions) becomes increasingly more saline due to volatile (CO_2) separation, and successively trapped inclusions during cooling, resulting from the formation and loss of high enthalpy steam, will show a liquid trend towards higher salinities, whereas the

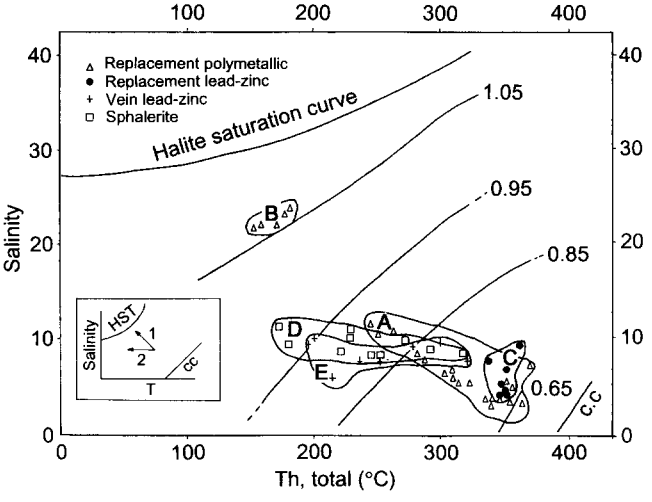

Fig. 7. Salinity (wt.% NaCl equivalent) versus T_h plot for quartz-hosted type I inclusions from the replacement polymetallic, replacement Pb-Zn and breccia/vein Pb-Zn ores, and sphalerite-hosted type I inclusions from the replacement polymetallic and replacement Pb-Zn ores. NaCl saturation curve (halite + liquid + vapor curve), selected isodensity curves (g/cm^3), and critical point curve (c.c.) of the system H_2O-NaCl are also shown (data from Sourirajan and Kennedy 1962; Urusova 1975; Haas 1976). *Inset diagram* is a schematic model showing boiling (1) and cooling, or "necking down" (2) trends of a liquid phase in terms of temperature and salinity (from Shepherd et al. 1985)

separated volatile phase (recorded in type II inclusions) will give rise to low-salinity "vapor"-rich inclusions (Hedenquist and Henley 1985; Ramboz et al. 1982; Shepherd et al. 1985). This trend can be seen clearly in Fig. 7 (field A) where the salinity of type I inclusions from polymetallic ore increases from 3.5 to 12 wt.% NaCl equivalent with a concomitant temperature decrease in the range from 380° to ~245 °C that coincides with the higher temperature population shown in Fig. 5A. The low salinity estimates of the coexisting type II inclusions (1–3.5 wt.% NaCl equivalent) are consistent with a boiling hypothesis.

Figure 7 also shows a group of inclusions (field B), which forms a higher salinity field near 21 to 24 wt.% NaCl equivalent, separated by a gap from the "boiling" trend, and corresponding to the lower temperature population from the polymetallic ore (Fig. 5A) between 150° and 220 °C. This temperature-salinity gap precludes boiling as the cause of the high salinity trend (field B) which may represent a late hydrothermal episode unrelated to the bulk of sulfide mineralization.

Overlapping temperature-salinity fields shown in Fig. 7 for all three ore varieties, in conjunction with the very similar salinity median values (Table 2), supports the suggestion made earlier that all three varieties belong to the same ore forming system.

Arrow number 2 from the inset diagram represents either a "necking down" trend that creates a spread in temperature with no significant change in salinity, or it may be due to simple cooling (Shepherd et al. 1985). Sphalerite-hosted type I inclusions, as well as inclusions in quartz from the breccia/vein ore, show the aforementioned trend (Fig. 7; fields D and E). In the absence of supporting evidence, trends due to "necking" or simple cooling are indistinguishable. Considering the extensive presence of "necked down" inclusions in sphalerite it may be concluded that the microthermometry trend observed in Fig. 7 is due to "necking down", and thus homogenization data of sphalerite are considered to be unreliable. This trend, however, may be explained by simple cooling for the breccia/vein ore due to the lack of obviously "necked" inclusions.

Pressure considerations. Evidence for immiscibility in fluid inclusions from samples of polymetallic ore eliminates the need for pressure correction to the T_h values which may be considered as the true trapping temperatures. More importantly, it permits a relatively accurate determination of pressure conditions, if both the temperature of trapping and the composition of the fluids are known.

Owing to the paucity of microthermometric data from the vapor-rich inclusions, the CO_2 content of type II inclusions cannot be quantified accurately. However, it may be presumed that the use of data obtained from spatially related liquid-rich type I inclusions adequately reflects conditions of the boiling fluid. The P-V-T data of Sourirajan and Kennedy (1962), Bodnar et al. (1985a) and Chou (1987) for the system H_2O-NaCl, combined with temperature and salinity data for type I inclusions, indicate maximum trapping pressures of less than 300 bar for trapping temperatures between 250° and 380 °C. These trapping (deposition) temperatures for the polymetallic ore are supported by independent formation temperature estimates of 250°–399 °C sphalerite-galena equilibrium sulfur isotope pairs (Changkakoti et al. 1990). The absence of type II inclusions from all samples of the polymetallic ore indicates that generally the total pressure on the fluid was higher than the boiling pressure. However, the excellent fit of the highest inclusion homogenization temperatures with the highest deposition temperatures determined from sulfur isotopes indicate that no significant pressure correction is probably required, and that a maximum formation pressure of 300 bar is acceptable for the polymetallic ore. The lower homogenization temperature population of polymetallic ore shown in Fig. 5A, between 150° and 220 °C most probably reflects quartz precipitation after the bulk of sulfide deposition.

No evidence for fluid boiling has been found in the replacement Pb-Zn and breccia/vein ores. Therefore, fluid inclusion trapping pressures were greater than the minimum vapor pressure that provides a minimum pressure estimate for the ore-fluid. Minimum pressures determined for type I inclusions from replacement Pb-Zn and breccia/vein ore (Sourirajan and Kennedy 1962) are 75 to 135 bar and 25 to 75 bar respectively.

In summary, the pressure estimates for the Thermes ore-forming system vary from less than 75 bar for the breccia/vein ore to 75–300 bar for the replacement ores. Considering the overlap between the fluid inclusion T_h values of both replacement ore varieties and temperatures derived from sulfur isotopes (Changkakoti et al. 1990), trapping pressures for the replacement Pb-Zn and replacement polymetallic ores are likely similar. For a maximum pressure of 300 bar, and the range of salinities recorded in this study, the pressure correction to homogenization temperatures of 190 °C to 380 °C should not exceed 40 °C (Potter 1977). Therefore, no attempt has been made to correct the T_h data from Thermes for pressure.

Fluid inclusions: Thermes versus other deposits

Figure 8 shows plots of fluid inclusion salinity (wt.% NaCl equivalent except Uchucchacua: in wt.% $NaCl + CaCl_2$ equivalent versus total homogenization temperature data from Thermes in comparison to other similar deposits such as Madan, skarn-type Pb-Zn replacement ores (Naica, Providencia, Groundhog, Washington Camp, Hidalgo), vein replacement and skarn Ag-Mn-Pb-Zn ores (Uchucchacua-fluid inclusion data are from replacement and vein ores only), carbonate-replacement skarn-free Pb-Zn (Ag ± Au) ores (Olympias, Taebaek, Bluebell), and epithermal polymetallic Ag-Pb-Zn (Ag) ores (Creede, Finlandia, Sunnyside) (for references see Fig. 8 caption). The data field of Thermes overlap (actually contains) that of Madan, and intersects those of the skarn-free carbonate replacement and epithermal envir onments. The reason for the intersecting relations is that salinity-temperature gradients in these deposition environments, excluding Olympias, have been ascribed to fluid mixing, producing positive correlation trends between decreasing salinity and temperature. The gradients for Thermes have been derived from fluid boiling and/or simple cooling that produce a progressive salinity increase

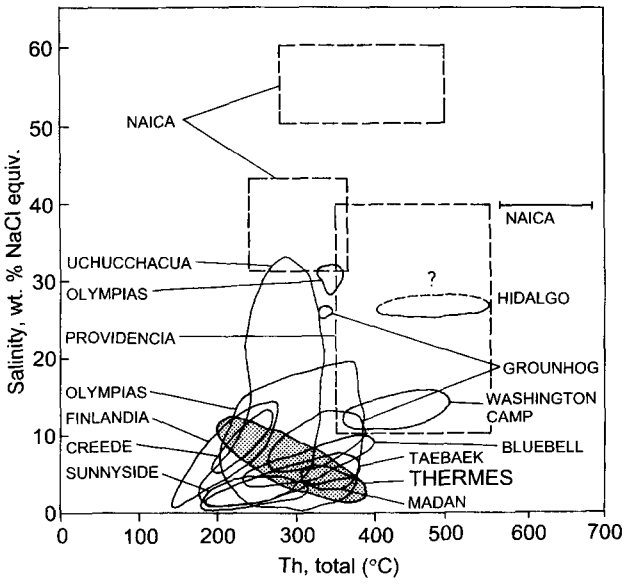

Fig. 8. Comparison of fluid inclusion salinity (wt.% NaCl equivalent) versus total homogenization temperatures (°C) plots of Thermes with Madan, Bulgaria (Piperov et al. 1977), Pb-Zn skarn-type deposits (Naica, Mexico (Erwood et al. (1979) and Megaw et al. 1988), Providencia, Mexico (Sawkins (1964) and Megaw et al. 1988), Groundhog, USA (Meinert 1987), Washington Camp, USA (Surles (1978) in Kwak 1986), Hidalgo, Mexico (Simone (1951) in Kwak 1986), Uchucchacua, Peru (Bussel et al. 1990), carbonate-replacement skarn-free Pb-Zn (Ag ± Au) deposits [Taebaek, Korea (So et al. 1993), Bluebell, Canada (Ohmoto and Rye 1970), Olympias, Greece (Kilias and Konnerup-Madsen 1994)], epithermal polymetallic Ag-Pb-Zn (Au) deposits [(Creede, USA (Woods et al. (1982) in Hedenquist and Henley 1985), Finlandia, Peru (Kamilli and Ohmoto 1977), Sunnyside, USA (Casadevall and Ohmoto 1977)]

trend during volatile separation and cooling, and a cooling temperature spread with no significant salinity change. In the case of Olympias, the salinity-temperature trend has been ascribed to a complex overprinting of fluid boiling and mixing (Kilias and Konnerup-Madsen 1994). These comparative fluid inclusion data indicate that the Thermes ores have been deposited under pressure conditions similar to those recorded in Madan (*P*: 100 bar), the carbonate-replacement Taebaek (*P*: 210–420 bar), Bluebell (*P*: 300–800 bar), Olympias ($P < 500$ bar), the epithermal Sunnyside (*P*: 110–220 bar), and the replacement bodies of Uchucchacua (*P*: 160–425 bar).

Isotopic evidence

Lead isotope data indicate that the Thermes ore lead was derived mainly from pre-existing evolved crustal material (Changkakoti et al. 1990). Moreover, lead isotopic ratios for galena from Thermes ores indicate model ages of 70 to 90 Ma, with a mean of 80 Ma, whereas those reported by Amov et al. (1991) and Arvanitidis (1993) span 18 to 30 Ma. These ages overlap and postdate the regional prograde amphibolite metamorphic event (Upper Cretaceous to Early/Middle Eocene).

Data obtained in a regional study of lead isotope composition in ore galena and feldspar from metamorphic rocks and granites of the Rhodope region in Bulgaria

Table 3. Stable isotope data of Thermes and Madan deposits

		Thermes[a]	Madan[b]
Sulfur isotopes	Minerals analyzed	ga,sph,py,cpy	ga,sph,cpy,po
	$\delta^{34}S$ (‰ CDT)	− 0.8 to 6.1	0.0 to 7.5
	Isotopic T (°C) (Sph-ga)	265 − 399	260 − 355
	Source	Igneous	Premetamorphic Sulfides (?)
Oxygen isotopes	$\delta^{18}O_{fluid}$ (‰ SMOW)		− 17.0 to 0.0[c] − 5.0 to 0.0[d]
	Source		Meteoric
Hydrogen isotopes	δD_{fluid} (‰ SMOW)		− 62.4 ± 7[c]
	Source		Meteoric

[a] Data of Changkakoti et al. (1990)
[b] Data of Bonev et al. (1993); Piperov and Penchev (1982)
[c] Fluid inclusion H_2O in ga;
[d] calculated from $\delta^{18}O_{quartz}$
ga: galena, sph: sphalerite, py: pyrite, cpy: chalcopyrite, po: pyrrhotite

(Marchev et al. 1990; Amov et al. 1991) indicate that: (1) a similar pre-existing evolved crustal material is involved in the formation of the Upper Cretaceous (90–70 Ma) and Paleocene (50–20 Ma) granites; (2) the ore lead values are comparable with those from feldspar leads from these granites. Considering the fact that the RM in Greece and Bulgaria share common geological characteristics and evolution, it is reasonable to assume that these conclusions hold true for the Greek RM also. Thus, the source of lead may be granitic stocks. As the granitic stocks in the Thermes area are of Oligocene age, this may also be considered as the most likely age for the formation of the Thermes ores.

Uniform sulfur isotope systematics and sulfur isotopic temperatures, compositional data for ore-fluids and deposition conditions for Thermes and Madan deposits (Table 3; Fig. 8), coupled with geological and mineralogical similarities (Manev et al. 1990), indicate a common source of ore-forming fluids for the Madan-Thermes ore district. Based on O, H, and S isotopes (Changkakoti et al. 1990; Bonev et al. 1993) a meteoric-hydrothermal convective ore-forming system driven by the Tertiary igneous activity is suggested for the entire Thermes-Madan orefield. However, due to the igneous signature of sulfur and lead isotopes (Changkakoti et al. 1990; Marchev et al. 1990; Amov et al. 1991) a magmatic contribution to the ore-forming system cannot be discounted.

Thermochemical considerations

Chemical changes of the hydrothermal fluids during deposition of the three ore varieties were calculated using equilibrium thermodynamics.

Fugacity of sulfur

The mol % FeS content of sphalerite from the three ore varieties were used to calculate the fugacity of sulfur in the

Fe-Zn-S system (Czamanske 1974; Scott and Barnes 1971). The range of log f_{S_2} at the temperatures obtained from fluid inclusions are: replacement polymetallic, − 14.1 to − 6.1 atm; replacement Pb-Zn, − 10.2 to − 6.1 atm; breccia/vein Pb-Zn, −13.6 to −5.5 atm.

O_2, CO_2, and H_2S fugacities

The stability relations among Fe, Mn, and Ca minerals were used in conjunction with thermochemical data from Helgeson (1969) and Robie et al. (1978) in order to calculate the fugacities of O_2, CO_2, and H_2S. The probable f_{O_2} and f_{CO_2} ranges were determined for 200°, 300° and 350 °C. (Fig. 9). Magnetite and alabandite do not occur in the Thermes ores, whereas graphite occurs in the host marbles. The estimated ranges of log f_{O_2} and log f_{CO_2} values for each ore variety are as follows: replacement polymetallic (at 200°–350 °C), log f_{O_2} = − 44.1 to − 28.1, log f_{CO_2} = − 1.3 to 4.4; replacement Pb-Zn (at 300° to 350 °C), log f_{O_2} = −34.6 to − 28.1, log f_{CO_2} = 0.7 to 4.4, breccia/vein (at 200° to 300 °C), log f_{O_2} = − 44.1 to − 33.2, log f_{CO_2} = − 1.3 to 2.8.

The ranges of the f_{H_2S} values were estimated at the above temperatures based on the reaction $H_2S + 1/2\ O_2 = H_2O + 1/2\ S_2$ and using the equilibrium constants of Helgeson (1969). Under the calculated f_{S_2} and f_{O_2} conditions for each ore variety, the average log f_{H_2S} values are as follows: replacement polymetallic, −3.6 to −1.3; replacement Pb-Zn, −3.5 to −0.08; breccia/vein, −3.0 to +0.3.

pH values

On the basis of fluid inclusion salinity data, the molal concentration of dissolved salts in the Thermes mineralizing fluids were calculated as follows: replacement polymetallic, 0.6–4.0 *m*; replacement Pb-Zn, 0.9–1.7 *m*; breccia/vein, 1.1–1.8 *m*. Assuming that the fluids consist essentially of H_2O and NaCl (see fluid inclusion Sect.), the ionic strength (I) of the fluids may be calculated using the data of molality of salts. The average ionic strength of the fluids for each ore variety is: replacement polymetallic, 2.3; replacement Pb-Zn, 1.3; breccia/vein, 1.4. The delta approximation method in Helgeson (1969) was used in the calculations.

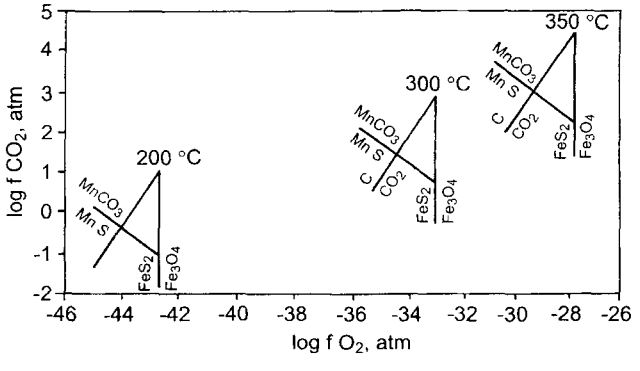

Fig. 9. Fugacity of CO_2 versus fugacity of O_2 showing stability relationships at 350°, 300° and 200 °C. Data from Helgeson (1969) and Robie et al. (1978)

The presence of sericite together with the equilibrium constants (Helgeson 1969) for the reaction K feldspar + H^+ = muscovite + quartz + K^+ set the pH conditions of the fluids. The probable concentrations of K^+ in the fluids for each ore variety was approximated using the data on K/Na ratios versus temperature for modern geothermal waters (Fournier and Truesdell 1973), as in the Thermes mineralizing process evolved local meteoric waters probably were mixed with magmatic fluids (see isotopic evidence and fluid inclusion Sect.). The estimated molal concentrations of K^+ for each ore variety at Thermes range as follows: replacement polymetallic, 0.3 to 1.1; replacement Pb-Zn, 0.33 to 0.5; breccia/vein, 0.2 to 0.4. Therefore, if the pH value of the ore-forming fluids was initially controlled at depth by the silicate assemblage quartz + sericite + K feldspar in granitic rocks, then the initial pH conditions of ore formation could be estimated to be about 3.8 to 4.8; 4.1 to 4.4; and 4.3 to 4.9, respectively for each ore variety.

As the hydrothermal fluids achieved equilibrium with the host "limestone" new sets of reactions governed the chemical conditions. Using the estimated minimum log f_{CO_2} values of 2.1, 0.7, − 1.3 respectively at 350°, 300° and 200 °C, the calcite equilibria as described in Ohmoto (1972, Eq. 61) can be used to define the upper limits of the pH values. The calculated pH values are as follows: replacement polymetallic, pH = 6 at 350 °C and $m_{\Sigma C}$ = 0.1; replacement Pb-Zn, pH = 6.3 at 300 °C and $m_{\Sigma C}$ = 0.034, breccia/vein, pH = 7.1 at 200 °C and $m_{\Sigma C}$ = 0.001 moles/kg H_2O. In summary, the pH values at Thermes could have increased from 3.8 to 7.1 for the replacement polymetallic ore, from 4.1 to 6.3 for the replacement Pb-Zn ore and from 4.3 to 6.3 for the breccia/vein ore.

Summary

Sulfide ore mineralization in the Thermes field consists of fault-related breccia/vein Pb-Zn mineralization, and strata-bound marble replacements with associated veins (Arvanitidis et al. 1986, 1989b). The latter are subdivided to polymetallic and Pb–Zn ore varieties. Cu-Pb-Zn, Cu-Pb + Zn-Ag × 10^3 bulk ore chemistries, regardless of ore type point to the similarity of the Thermes mineralizations with a skarn-replacement ore system, that is consistent with field and fluid inclusion data.

Coexisting aqueous liquid-rich (type I) inclusions and vapor-rich, CO_2-bearing (type II) inclusions in quartz in replacement polymetallic ore homogenize between 250° and 400 °C, and were trapped during fluid unmixing of a homogeneous aqueous CO_2-bearing, saline hydrothermal fluid, at pressures below 300 bar. Successive entrapment of a moderately saline liquid phase during volatile separation (CO_2), and cooling, accounts for the large salinity range of type I inclusions from 3.5 to 22.4 wt.% NaCl equivalent, and homogenization temperatures down to 250 °C. Microthermometry data of type I inclusions in the replacement Pb-Zn and breccia/vein ores indicate deposition at temperatures ranging from approximately 300° to 360 °C, and 200° to 320 °C, respectively, and pressures ranging between 25 and 300 bar.

An evolved meteoric fluid component is envisaged to have been involved, probably along with magmatic fluid contributions, in the Thermes ore-forming system.

Pressure and temperature conditions of ore deposition (P = 25–300 bar, $T \sim 200°$–400 °C) are significantly different from those corresponding to the regional amphibolite facies metamorphic conditions that affected the host lithologies (P = 5–7 kbar, T = 580°–620 °C). A postmetamorphic epigenetic origin is proposed for the Thermes ores.

Calculated geochemical parameters such as f_{S_2}, f_{O_2} and f_{H_2S} indicate that ore forming fluids varied mainly with a drop in temperature. The pH values of the mineralizing fluids were initially controlled by the quartz + sericite + K feldspar mineral assemblage at depth. As the mineralizing fluids reacted with the host marbles new sets of reactions are envisaged to have governed the pH conditions. Calculations of the calcite equilibria indicate that the pH of the ore-forming fluids was increased by at least two units due to fluid-carbonate interaction.

Most efficient mechanisms of ore deposition are considered a pH increase due to fluid-rock interaction, and adiabatic cooling and/or simple cooling accompanying fluid boiling.

References

Alfieris, D., Arvanitidis, N.D., Katirtzoglou, K. (1989) Petrology and geochemistry of acid dyke-rocks in the East Rhodope, Esimi area. Geol. Rhodopica 1:268–279

Amov, B., Arvanitidis, N.D., Constantinides, D.C. (1991) Isotopic composition of lead in galenas from some mineralizations in Greece and their interpretation. Unpubl. Rep. IGME, Thessaloniki Branch, 10 pp

Arvanitidis, N.D., Favas, N., Dimadis, E., Zanas, I., Kalogeropoulos, S.I. (1986) Zn-Pb-Cu sulfide mineralizations in the area of Thermes, Central Rhodope massif. Summary of preliminary geologic, petrologic and geochemical considerations. Unpubl. Final Rep., EEC-Rhodope R&D project, IGME, Athens, Greece, 47 pp

Arvanitidis, N.D., Dimadis, E., Favas, N., Zanas, I. (1989a) The geology, mineralogy, and petrogenesis of metamorphic rocks from the area of Thermes, Central Rhodope massif. 1st Hellenic-Bulgarian Symposium on the Geology and Physical Geography of the Rhodope Massif, Univ. Sofia. Geol. Rhodopica 1:169–185

Arvanitidis, N.D., Kalogeropoulos, S.I., Favas, N. (1989b) Zn-Pb-Cu sulfide mineralization in the area of Thermes, Central Rhodope Massif. Geol. Rhodopica 1:306–321

Arvanitidis, N.D., Dimou, E. (1990) Electrum and silver telluride occurrences in the polymetallic sulfide mineralization of the Thermes ore-field, N. Greece. 2nd Hellenic-Bulgarian Symp. Geology and Physical Geography of the Rhodope Massif, University of Thessaloniki. Geol. Rhodopica 2:309–325

Arvanitidis, N.D. (1993) Regional ore geologic studies: Setting controls and distribution of metallic deposit types in the Serbo-Macedonian and Western Rhodope zone. EEC project MA2M-CT90-0015 "Carbonate-hosted precious and base metal mineralization in Greece. Development of new exploration strategies", IGME, Thessaloniki, 99 pp

Barton, P.B., Jr., Toulmin, P., (1966) Phase relations involving sphalerite in the Fe-Zn-S system. Econ. Geol. 61:815–849

Bodnar, R.J., Burnham, C.W., Sterner, S.M. (1985a) Synthetic fluid inclusions in natural quartz. III. Determination of phase equilibrium properties in the system H_2O-NaCl to 1000 °C and 1500 bar. Geochim. Cosmochim. Acta 49:1861–1873

Bodnar, R.I., Reynolds, T.J., Kuehn, C.A. (1985b) Fluid inclusion systematics in epithermal systems. In: Berger, B.R., Bethke, P.M. (eds.) Geology and Geochemistry of epithermal systems. Rev. Econ. Geol. 2:73–97

Bonev, I.K., Boyce, A.J., Fallick, A.E., Rice, C.M. (1993) Stable isotope evidence for the genesis of the Madan vein and replacement Pb–Zn deposits, Central Rhodopes, Bulgaria. In: Fenoll Hach-Ali, P., Torres-Ruiz, J., Gevilla, F. (eds.) Current research in Geology Applied to Ore Deposits, Proc second biennial SGA meeting, Granada, Sept. 1993, pp. 37–40

Bowers, T.S., Helgeson, H.C. (1983) Calculation of the thermodynamic and geochemical consequences of nonideal mixing in the system H_2O-CO_2-NaCl on phase relations in geological systems: equation of state for H_2O-CO_2-NaCl fluids at high pressures and temperatures. Geochim. Cosmochim. Acta 47:1247–1275

Brown, P.E. (1989) FLINCOR: a microcomputer program for the reduction and investigation of fluid-inclusion data. Am. Mineral. 74:1390–1393

Brown, P.E., Lamb, W.M. (1989) P-V-T properties of fluids in the system $H_2O \pm CO_2 \pm$ NaCl: new graphical presentations and implications for fluid inclusion studies. Geochim. Cosmochim. Acta 53:1209–1221

Bussel, M.A., Alpers, C.N., Petersen, U., Shepherd, T.J., Bermudez, C., Baxter, A.N. (1990) The Ag-Mn-Pb-Zn vein, replacement and skarn deposits of Uchucchacua, Peru: studies of structure, mineralogy, metal zoning, Sr isotope fluid inclusions. Econ. Geol. 85:1348–1383

Casadevall, T., Ohmoto, H. (1977) Sunnyside mine, Eureka mining district, San Juan, Colorado: geochemistry of gold and base metal ore deposition in a volcanic environment. Econ. Geol. 72:1285–1320

Changkakoti, A., Dimitrakopoulos, R., Gray, J., Krouse, H.R., Krstic, D., Kalogeropoulos, S.I., Arvanitidis, N.D. (1990) Sulfur and lead isotopic composition of sulfide minerals from Thermes and Esimi, Rhodope Massif, Greece, Neues Jahrb. Mineral. Monatsh. 9:413–430

Chou, M.I. (1987) Phase relations in the system NaCl-KCl-H_2O. III: solubilities of halite in vapor-saturated liquids above 445 °C and redetermination of phase equilibrium properties in the system NaCl-H_2O to 1000 °C and 1500 bars. Geochim. Cosmochim. Acta 51:1965–2075

Collins, P.L.F. (1979) Gas hydrates in CO_2-bearing fluid inclusions and the use of freezing data for estimation of salinity. Econ. Geol. 74:1435–1444

Crawford, M.L. (1981) Phase equilibria in aqueous fluid inclusions. In: Hollister, L.S., Crawford, M.L. (eds.) Short course in fluid inclusions: applications to petrology. Min. Assoc. Can., pp. 75–97

Czamanske, G.K. (1974) The FeS content of sphalerite along the chalcopyrite-pyrite-bornite sulfur fugacity buffer. Econ. Geol. 69:1328–1334

Einaudi, M.T., Meinert, L.D., Newberry, R.J. (1981) Skarn deposits. Econ. Geol. 75th Anniv. Volume, pp. 317–391

Eleftheriadis, G., Christofides, G., Mavroudchiev, B., Nedyalkov, R., Andreev, A., Hristov, L. (1989) Tertiary volcanics from the East Rhodope in Greece and Bulgaria. Geol. Rhodopica 1:202–217

Erwood, R.J., Kesler, S.E., Cloke, P.L. (1979) Compositionally distinct, saline hydrothermal solutions, Naica mine, Chihuahua, Mexico. Econ. Geol. 74:95–108

Fournier, R.O., Truesdell, A.H. (1973) An empirical Na-K-Ca geothermometer for natural waters. Geochim. Cosmochim. Acta 37:1255–1275

Franklin, J.M., Lydon, J.W., Sangster, D.F. (1981) Volcanic-associated massive sulfide deposits. Econ. Geol. 75th Anniv. Volume, pp. 485–624

Fytikas, M., Innocenti, F., Manneti, P., Mazzuoli, R., Pesserillo, G., Villari, L. (1985) Tertiary to quaternary evolution of the volcanism in the Aegean region. In: Dixon, J.E., Robertson, A.H.F. (eds.) The geological evolution of the Eastern Mediterranean, Spec. Publ. Geol. Soc., 17. Blackwells, Oxford, pp. 687–699

Gustafson, L.B., Williams, N. (1981) Sediment-hosted stratiform deposits of copper, lead and zinc. Econ. Geol. 75th Anniv. Volume, pp. 139–178

Hass, J.L., Jr. (1976) Physical properties of the coexisting phases and thermochemical properties of the H_2O component in boiling NaCl solutions. US Geol. Surv. Bull., 1421-A, 73 pp

Helgeson, H.C. (1969) Thermodynamics of hydrothermal systems at elevated temperatures and pressures. Am. J. Sci. 267:729–804

Hedenquist, J.W., Henley, R.W. (1985) The importance of CO_2 freezing point measurements of fluid inclusions: Evidence from geothermal systems and implications for epithermal ore deposition. Econ. Geol. 80:1379–1406

Kalogeropoulos, S.I., Arvanitidis, N.D. (1989) A comparison of the chemistry of sphalerites between the Pb-Zn (Au-Ag) sulfide deposits of the eastern Chalkidiki Peninsula and the respective mineralization of the Thermes area, Xanthi, Geol. Soc. Greece Bull. 23:245–260

Kamilli, R.J., Ohmoto, H. (1977) Paragenesis, zoning, fluid inclusion and isotopic studies of the Finlandia vein, Colqui District, Central Peru. Econ. Geol. 72:950–982

Kilias, S.P., Konnerup-Madsen, J. (1994) H_2O-CO_2-NaCl fluid immiscibility: a mechanism for sulfide deposition in the Olympias Pb-Zn (Au, Ag) sulfide deposit, E. Chalkidiki, Macedonia, Greece. 7th Congress Geol. Soc. Greece, May 1994, Thessaloniki, Greece

Kokkinakis, A. (1980) Altersbeziehungen swischen Metamorphosen, mechanismen, deformationen and intrusionen and Sudrand, des Rhodope-Massives (Makedonien, Griechenland). Geol. Rundsch. 69.3:726–744

Kretschmar, V., Scott, S.D. (1976) Phase relations involving arsenopyrite in the system Fe-As-S and their application. Can. Mineral. 14:364–386

Kwak, T.A.P. (1986) Fluid inclusions in skarns (carbonate replacement deposits). J. Metam. Geol. 4:363–384

Kyriakopoulos, K. (1987) A geochronological, geochemical and mineralogical study of some Tertiary plutonic rocks of the Rhodope massif and their isotopic characteristics. Unpubl. Ph.D. Thesis, University of Athens, 343 pp. (in Greek)

Liati, A. (1986) Regional metamorphism and overprinting contact metamorphism of the Rhodope zone, near Xanthi (N. Greece). Petrology, geochemistry, geochronology. Unpubl. Ph.D. Thesis, Techn. University of Braunschweig, 186 pp

Lydon, J.W. (1983) Chemical parameters controlling the origin and deposition of sediment-hosted stratiform lead-zinc deposits. Mineral. Assoc. Can. 9:175–245

Macdonald, A.J., Spooner, E.T.C. (1981) Calibration of a LinkamTH600 programmable heating-cooling stage for microthermometric examination of fluid inclusions. Econ. Geol. 76:1248–1258

Manev, D., Katzkov, N., Milev, V., Malinov, D., Arvanitidis, N.D., Constantinides, D.C., Dimadis, E., Romaidis, N., Favas, N. (1990) Comparison between Madan (Bulgaria) and Thermes (Greece) ore fields. Geology and metallogenesis. 2nd Hellenic-Bulgarian Symp. Geology and Physical Geography of the Rhodope Massif, University of Thessaloniki. Geol. Rhodopica 2:309–325

Marchev, P., Lilov, P., Amov, B. (1990) Major, trace-element and isotopic (Sr, Pb) zonality in the Eocene-Oligocene Macedonian-Rhodope magmatic zone: evidence for WPB-like source, subduction processes and crustal influence. 2nd Hellenic-Bulgarian Symp. Geology and Physical Geography of the Rhodope Massif, University of Thessaloniki, Abstr. pp. 41

Megaw, P.K.M., Ruiz, J., Titley, S.R. (1988) High-temperature carbonate-hosted Ag-Pb-Zn (Cu) deposits of Northern Mexico. Econ. Geol. 83:1856–1885

Meinert, L.D. (1987) Skarn zonation and fluid evolution in the Groundhog mine, Central Mining District, New Mexico. Econ. Geol. 82:523–545

Meyer, W. (1968) Zur alterstellumg des plutonismus im Sudteil der Rila-Rhodope masse (Nordgrienchenland). Geol. Palaeontologica 2:173–192

Mposkos, E., Liati, A., Katagas, C., Arvanitidis, N.D. (1990) Petrology of the metamorphic rocks of West Rhodope, Drama area, N. Greece. 2nd Hellenic-Bulgarian Symp. Geology and Physical Geography of the Rhodope Massif, University Thessaloniki. Geol. Rhodopica 2:127–142

Ohmoto, H. (1972) Systematics of sulfur and carbon isotopes in hydrothermal ore deposits. Econ. Geol. 67:557–578

Ohmoto, H., Rye, R.O. (1970) The Bluebell mine, British Columbia. I. Mineralogy, paragenesis, fluid inclusions, and the isotopes of hydrogen, oxygen, and carbon, Econ. Geol. 65:417–437

Piperov, N.B., Penchev, N.B., Bonev, I.K. (1977) Primary fluid inclusions in galena crystals. II. Chemical composition of the liquid and gas phase. Mineral. Deposita. 12:77–89

Piperov, N.B., Penchev, N.P. (1982) Deuterium content of the inclusion water from hydrothermal galenas, Madan, Bulgaria: preliminary investigation. Econ. Geol. 77:195–197

Potter, R.W., II (1977) Pressure corrections for fluid inclusion homogenization temperatures based on the volumetric properties of the system NaCl-H_2O. US Geol. Surv. J. Res. 5:603–607

Potter, R.W., II, Clynne, M.A., Brown, D.L. (1978) Freezing point depression of aqueous sodium chloride solutions. Econ. Geol. 73:284–285

Ramboz, C., Pichavant, M., Weisbrod, A. (1982) Fluid immiscibility in natural processes: use and misuse of fluid inclusion data. Chem. Geol. 37:29–48

Robie, R.A., Hemingway, B.S., Fisher, J.R. (1978) Thermodynamic properties of minerals and related substances at 298.15 K and 1 bar (10^5 pascals) pressure and at higher temperatures. US Geol. Surv. Bull. 1452, 456 pp

Roedder, E. (1984) Fluid inclusions. Mineral. Soc. Am., Reviews in Mineralogy 12, 644 pp

Sawkins, F.J. (1964) Lead-zinc ore deposition in the light of fluid inclusions, Providencia mine, Zacatecas, Mexico. Econ. Geol. 59:883–919

Sangster, D.F., Scott, S.D. (1976) Precambrian stratabound, massive Cu-Zn-Pb sulfide ores of North America. In: Wolf, K.H. (ed.) Handbook of strata-bound and stratiform ore deposits. Elsevier, Amsterdam, pp. 129–222

Scott, S.D., Barnes, H.L. (1971) Sphalerite geothermometry and geobarometry. Econ. Geol. 66:653–669

Shepherd, T.J. (1981) Temperature programmable heating-freezing stage for microthermometric analysis of fluid inclusions. Econ. Geol. 76:1244–1247

Shepherd, T.J., Rankin, A.H., Alderton, D.H.M. (1985) A practical guide to fluid inclusion studies. Blackie, New York, 239 pp

Simone, I.S. (1951) Geology and ore deposits of the Zimapan mining district, Mexico. Unpubl. Ph.D. Thesis, Stanford University, 237 pp

Sklavounos, S. (1981) The Paranesti granite (Mineralogy-Petrography). Unpubl. Ph.D. Thesis, Univ. of Thessaloniki, Greece, 175 pp. (in Greek)

So, C., Yun S., Koh, Y. (1993) Mineralogic, fluid inclusion, and stable isotope evidence for the genesis of carbonate-hosted Pb-Zn (-Ag) orebodies of the Taebaek deposit, Republic of Korea. Econ. Geol. 88:855–872

Sourirajan, S., Kennedy, G.C. (1962) The system H_2O-NaCl at elevated temperatures and pressures. Am. J. Sci. 260:115–141

Surles, T.L. (1978) Chemical and thermal variations accompanying formation of garnet skarns near Patagonia, Arizona. Unpubl. M.Sc. Thesis, University of Arizona, 54 pp

Urusova, M.A. (1975) Phase equilibria and thermodynamic characteristics of solutions in the system H_2O-NaCl and NaOH-H_2O 350–550 °C. Geochem. Int. 11:944–950

Von Braun, E. (1993) The Rhodope question viewed from eastern Greece. Z. Dtsche. Geol. Ges. 144:406–418

Woods, T.L., Roedder, E., Bethke, P.M. (1982) Fluid inclusion data on samples from Creede, Colorado, in relation to mineral paragenesis. US Geol. Surv. Open-File Rep. 82-313, 77 pp

Yordanov, N., Vergilov, V., Pavlova, M. (1962) Geological age of the crystalline complex and the granitoids in South Bulgaria, determined after the K/Ar method. Bull Strasimir Dimitrov Inst. Geol. 11:33–39

Editorial handling: K. Shelton